Proceedings, Bicycle and Motorcycle Dynamics 2010
Symposium on the Dynamics and Control of Single Track Vehicles,
20 - 22 October 2010, Delft, The Netherlands

Modeling of a Motorcycle Using Multi-Body Dynamics and Its Stabilization Control

S. Murakami [*], S. Zhu [#], H. Nishimura [†]

[*] Graduate School of System Design and Management
Keio University
4-1-1 Hiyoshi, Kohoku-ku, 223-8526 Yokohama, Japan
e-mail: s.murakami@z5.keio.jp

[#] School of Medicine
Keio University
35 Shinanomachi, 160-8582 Shinjuku-ku, Tokyo, Japan
e-mail: zspsdm@a5.keio.jp

[†] Graduate School of System Design and Management
Keio University
4-1-1 Hiyoshi, Kohoku-ku, 223-8526 Yokohama, Japan
e-mail: h.nishimura@sdm.keio.ac.jp

ABSTRACT

In this paper, a new rider-motorcycle system including front and rear suspensions is modeled using multi-body dynamics, and the stabilization control system is designed for the linearized reduced-order model. We have already modeled the rider-motorcycle system taking into account of the lean angle of the rider's upper torso. The front and rear suspensions will be necessary for dynamical analysis of a motorcycle in braking situations. For the derived dynamical model with the front and rear suspensions, the front-steering assist controller is designed utilizing H_∞ control. By carrying out simulations, the driving stability of the rider-motorcycle system with the front-steering assist control is investigated.

Keywords: vehicle dynamics, motorcycle, front-steering assist control, modeling.

1 INTRODUCTION

Recently, electric stability control systems for four-wheel vehicles are well studied. A motorcycle may be required to implement one of these systems in the future. Realizing these systems will need not only wheel control but also stability control by front steering.

Detail simulation models for motorcycles have been developed based on Lagrange's equation of motion [1], [2], [3], and it enables simulation of motorcycle dynamics with a commercial software. On the other hand, analyzing the dynamical system for designing a control system often requires an appropriate reduced-order model. We have already modeled the rider-motorcycle system using multi-body dynamics [4] taking into account the lean angle of the rider's upper torso [5], [6]. It has been demonstrated that a front-steering assist control stabilizes the motorcycle against applied impulsive disturbance on the front wheel [5], [7], [8]. For driving in a straight line at a low speed, references [7] and [8] have experimentally verified the stabilization capability of the front-steering assist control. In braking situations, the front and rear suspensions will be necessary for dynamical analysis of a motorcycle.

In this paper, a new rider-motorcycle system including front and rear suspensions [1], [2], [3] is modeled. And the stabilization control system is designed for the linearized reduced-order model in steady-state circular turning. In particular, the driving stability of the rider-motorcycle system is investigated under the condition when the pitting motion is occurred due to braking.

2 MODELING

2.1 The Rider-Motorcycle System

The ten-degree of freedom rider-motorcycle system [5] includes the lean motion of the rider's upper torso: θ_{wx} rotating around the x-axis of the rear frame of the motorcycle, the steering angle: δ and the rotation of the front and the rear wheel. In addition to them, this model includes the compression angle of the rear suspension: ψ and the compression length of the front suspension: l_{UD}, which are restrained with a spring and a dumper respectively. The rider's upper torso is connected to the handle with a spring and a damper.

The dynamical model of the rider-motorcycle system is shown in Figure 1. It consists of five bodies; the rear frame (the rear frame, the rider's lower body, the engine and the fuel tank), the front frame (the front fork, the steering head and the handle bars), the rear wheel, the front wheel and the rider's upper torso. Table 1 shows specifications of the model [9]. The notations of Figure 1 are as follows; A: center of mass of the rear frame, U: center of mass of the front frame, C: center of mass of the rear wheel, D: center of mass of the front wheel, W: center of mass of the rider's upper torso, m_A: mass of the rear frame, m_U: mass of the front frame, m_D: mass of the rear wheel, m_A: mass of the front wheel, m_W: mass of the rider's upper torso, P_r: ground contact point of rear wheel, P_f: ground contact point of front wheel, λ: caster angle, τ_{rr}: driving/braking torque of rear wheel, τ_{rf}: driving/braking torque of rear wheel, τ_{rr}: braking torque of front wheel, and τ_f: steering torque. The center of mass of each rigid body is defined as the origin of each standard coordinate system.

The generalized coordinate and the generalized velocity are defined as

$$\begin{aligned}\mathbf{Q} &= \begin{bmatrix}\mathbf{R}_{OA}{}^{T} & \mathbf{\Theta}_{OA}{}^{T} & \delta & \theta_{wx} & \theta_r & \theta_f & \psi & l_{UD}\end{bmatrix}^T \\ \mathbf{S} &= \begin{bmatrix}\mathbf{V}_{OA}{}^{T} & \dot{\mathbf{\Theta}}_{OA}{}^{T} & \dot{\delta} & \dot{\theta}_{wx} & \dot{\theta}_r & \dot{\theta}_f & \dot{\psi} & \dot{l}_{UD}\end{bmatrix}^T \quad ,\end{aligned} \tag{1}$$

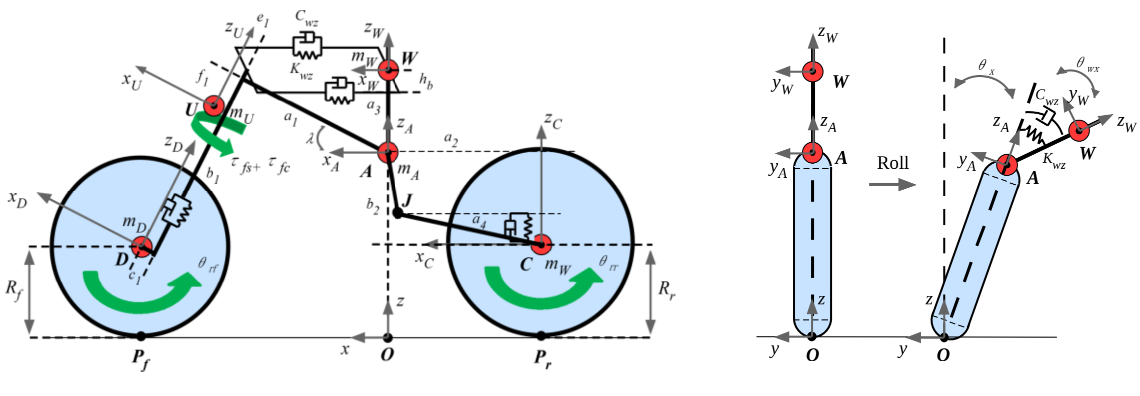

(a) Side view (b) Rear view

Figure 1. Dynamical model of rider-motorcycle system

Table 1. Specification of Motorcycle

Mass	m_A	m_U	m_W	m_C	m_D
[kg]	164.43	15.5	50	19.2	10.9
Inertia	I'_{OAxx}	I'_{OUxx}	I'_{OWxx}	I'_{OCxx}	I'_{ODxx}
	26.04	1.74	4.75	0.41	0.26
	I'_{OAyy}	I'_{OUyy}	I'_{OWyy}	I'_{OCyy}	I'_{ODyy}
[kgm^2]	24.73	0.3	0	1.68	0.47
	I'_{OAzz}	I'_{OUzz}	I'_{OWzz}	I'_{OCzz}	I'_{ODzz}
	26.28	0.4	4.75	0.41	0.26
Length	a_1	a_2	a_3	a_4	b_1
	0.545	0.523	0.357	0.50	0.707
[m]	b_2	c_1	f_1	e_1	R_r
	0.307	0.05	0.13	0.049	0.312
Spring	K_{wx}	K_{wz}	K_{cs}	K_{ds}	R_f
stiffness	350	172.2	40000	25000	0.299
	[Nm/rad]	[N/m]	[N/m]	[N/m]	
Damping	C_{wx}	C_{wz}	C_{cs}	C_{ds}	
coefficient	20	26.4	1000	2000	
	[Nms/rad]	[Ns/m]	[Ns/m]	[Ns/m]	

Where

$$\mathbf{R}_{OA}{}^{T} = \begin{bmatrix} x_A & y_A & z_A \end{bmatrix},\ \mathbf{\Theta}_{OA}{}^{T} = \begin{bmatrix} \theta_z & \theta_x & \theta_y \end{bmatrix} \quad .$$

The dynamical model has twelve degrees of freedom: the position $\mathbf{R}_{OA}$ of the rear frame in the inertia coordinate system, the Euler angles $\mathbf{\Theta}_{OA}$ of the rear frame, the steering angle δ, the roll angle of the rider's upper torso θ_{wx}, the rotation angle of the rear wheel θ_{rr}, the rotation angle of the front wheel θ_{rf}, this model includes the compression angle of the rear suspension ψ, the compression length of the front suspension: l_{UD}.

Let $\boldsymbol{C}_{OA}$ be a rotation matrix that completes the rotation of a vector from the inertia coordinate system to the A coordinate system. Then the relationship between the derivative of the generalized coordinate and the generalized velocity is given as follows

$$\dot{\mathbf{Q}} = \frac{\partial H}{\partial \mathbf{S}} \mathbf{S} = \begin{bmatrix} \mathbf{C}_{OA} & \mathbf{O}_{3\times 9} \\ \mathbf{O}_{9\times 3} & \mathbf{I}_9 \end{bmatrix} \cdot \mathbf{S} \quad . \tag{2}$$

Introducing velocity vectors:

$$\mathbf{\Lambda}'_{Oi} = \begin{bmatrix} \mathbf{V}'^{T}_{Oi} & \mathbf{\Omega}'^{T}_{Oi} \end{bmatrix}^{T}, \quad (i : A,\ U,\ C,\ D \text{ and } W) \tag{3}$$

and the angular velocity vectors:

$$
\begin{aligned}
\mathbf{\Omega}_{OA} &= \mathbf{M}_{OA} \cdot \dot{\mathbf{\Theta}}_{OA} \\
&= Cy(\theta_y)^{-1} \cdot Cx(\theta_x)^{-1} \cdot \mathbf{e}_z \cdot \dot{\theta}_z + Cy(\theta_y)^{-1} \cdot \mathbf{e}_x \cdot \dot{\theta}_x + \mathbf{e}_y \cdot \dot{\theta}_y \\
\mathbf{\Omega}_{OU} &= C_{AU}^{-1} \cdot \mathbf{\Omega}_{OA} + \mathbf{e}_z \cdot \dot{\delta} \\
\mathbf{\Omega}_{OW} &= C_{AW}^{-1} \cdot \mathbf{\Omega}_{OA} + \mathbf{e}_x \cdot \dot{\theta}_{wx} \\
\mathbf{\Omega}_{OC} &= C_{JC}^{-1} \cdot C_{AJ}^{-1} \cdot \mathbf{\Omega}^{A} + \mathbf{e}_y \cdot (\dot{\psi} + \dot{\theta}_r) \\
\mathbf{\Omega}_{OD} &= C_{UD}^{-1} \cdot C_{AU}^{-1} \cdot \mathbf{\Omega}^{A} + C_{UD}^{-1} \cdot \mathbf{e}_z \cdot \dot{\delta} + \mathbf{e}_y \cdot \dot{\theta}_f
\end{aligned}
\tag{4}
$$

the velocity matrix H is obtained with Jacobian as Equation (5).

$$
\begin{aligned}
H &= \begin{bmatrix} \mathbf{\Lambda}_{OA}^T & \mathbf{\Lambda}_{OU}^T & \mathbf{\Lambda}_{OW}^T & \mathbf{\Lambda}_{OC}^T & \mathbf{\Lambda}_{OD}^T \end{bmatrix}^T \\
&= \begin{bmatrix}
I_3 & O_3 & O_{31} & O_{31} & O_{31} & O_{31} & O_{31} & O_{31} \\
O_3 & I_3 & O_{31} & O_{31} & O_{31} & O_{31} & O_{31} & O_{31} \\
C_{AU}^T & C_{AU}^T \cdot \tilde{\mathbf{R}}_{AU}^T & \mathbf{R}_{UH} \cdot \mathbf{e}_z & O_{31} & O_{31} & O_{31} & O_{31} & O_{31} \\
O_3 & C_{AU}^T & \mathbf{e}_z & O_{31} & O_{31} & O_{31} & O_{31} & O_{31} \\
C_{AW}^T & C_{AW}^T \cdot \tilde{\mathbf{R}}_{AW}^T & O_{31} & \tilde{\mathbf{R}}'^T_{AW} \cdot \mathbf{e}_x & O_{31} & O_{31} & O_{31} & O_{31} \\
O_3 & C_{AW}^T & O_{31} & \mathbf{e}_x & O_{31} & O_{31} & O_{31} & O_{31} \\
C_{AC}^T & C_{AC}^T \cdot \tilde{\mathbf{R}}_{AC}^T & O_{31} & O_{31} & O_{31} & O_{31} & C_{JC}^T \cdot \tilde{\mathbf{R}}_{JC}^T \cdot \mathbf{e}_y & O_{31} \\
O_3 & C_{AC}^T & O_{31} & O_{31} & \mathbf{e}_y & O_{31} & \mathbf{e}_y & O_{31} \\
C_{UD}^T \cdot C_{AU}^T & \begin{matrix} C_{UD}^T \cdot (C_{AU}^T \cdot \tilde{\mathbf{R}}_{AU}^T) \\ + C_{UD}^T \cdot (\tilde{\mathbf{R}}_{UD}^T \cdot C_{AU}^T) \end{matrix} & C_{UD}^T \cdot (-\tilde{\mathbf{R}}_{UH} + \tilde{\mathbf{R}}_{UD})^T \cdot \mathbf{e}_z & O_{31} & O_{31} & O_{31} & O_{31} & -C_{UD}^T \cdot \mathbf{e}_z \\
O_3 & C_{UD}^T \cdot C_{AU}^T & C_{UD}^T \cdot \mathbf{e}_z & O_{31} & O_{31} & \mathbf{e}_y & O_{31} & O_{31}
\end{bmatrix} \\
&\quad \cdot \begin{bmatrix} \mathbf{V}_{OA}^T & \mathbf{\Omega}_{OA}^T & \dot{\delta} & \dot{\theta}_{wx} & \dot{\theta}_r & \dot{\theta}_f & \dot{\psi} & \dot{l}_{UD} \end{bmatrix}^T
\end{aligned}
\tag{5}
$$

2.2 Forces and Torques of the Rigid Bodies

The forces $\mathbf{F}$ and the torques $\mathbf{N}$ to the rigid bodies are described as Equations (6) and (7) respectively.

$$
\begin{aligned}
\mathbf{F}'_{OA} &= C_{OA}^T \cdot \mathbf{F}_{OA} = -C_{OA}^T \cdot (m_A \cdot g \cdot \mathbf{e}_z) - \mathbf{F}_{AC} \\
\mathbf{F}'_{OU} &= C_{OU}^T \cdot \mathbf{F}_{OU} = -C_{OU}^T \cdot (m_U \cdot g \cdot \mathbf{e}_z) - \mathbf{F}_{UD} \\
\mathbf{F}'_{OW} &= C_{OW}^T \cdot \mathbf{F}_{OW} = -C_{OW}^T \cdot (m_W \cdot g \cdot \mathbf{e}_z) \\
\mathbf{F}'_{OC} &= C_{OC}^T \cdot \mathbf{F}_{OC} = -C_{OC}^T \cdot (m_C \cdot g \cdot \mathbf{e}_z + \mathbf{f}_{cpr}) + \mathbf{F}_{AC} \\
\mathbf{F}'_{OD} &= C_{OD}^T \cdot \mathbf{F}_{OD} = -C_{OD}^T \cdot (m_D \cdot g \cdot \mathbf{e}_z + \mathbf{f}_{cpf}) + \mathbf{F}_{UD}
\end{aligned}
\tag{6}
$$

$$
\begin{aligned}
\mathbf{N}'_{OA} &= (\tau_{xp} - \tau_{xa}) \cdot \mathbf{e}_x - \tau_{rr} \cdot C_{AC}{}^{-1} \cdot \mathbf{e}_y - \tau_{rf} \cdot C_{AD}{}^{-1} \cdot \mathbf{e}_y - \tilde{\mathbf{R}}_{AC} \cdot \mathbf{F}_{AC} \\
\mathbf{N}'_{OU} &= \tau_{zp} \cdot C_{WU}{}^{-1} \cdot \mathbf{e}_z - \tau_f \cdot \mathbf{e}_z + \tau_{rf} \cdot C_{UD}{}^{-1} \cdot \mathbf{e}_y - \tilde{\mathbf{R}}_{UD} \cdot \mathbf{F}_{UD} \\
\mathbf{N}'_{OW} &= -(\tau_{xp} - \tau_{xa}) \cdot \mathbf{e}_x - \tau_{zp} \cdot \mathbf{e}_z + \tau_f \cdot C_{WU} \cdot \mathbf{e}_z \\
\mathbf{N}'_{OC} &= \tau_{rr} \cdot \mathbf{e}_y + \tau_{zr} \cdot C_{OC}{}^{-1} \cdot \mathbf{e}_z + \tilde{\mathbf{R}}_{CP} \cdot C_{OC}{}^{-1} \cdot \mathbf{f}_{opp} \\
\mathbf{N}'_{OD} &= \tau_{rf} \cdot \mathbf{e}_y + \tau_{zf} \cdot C_{OD}{}^{-1} \cdot \mathbf{e}_z + \tilde{\mathbf{R}}_{CP} \cdot C_{OD}{}^{-1} \cdot \mathbf{f}_{oqq}
\end{aligned}
\tag{7}
$$

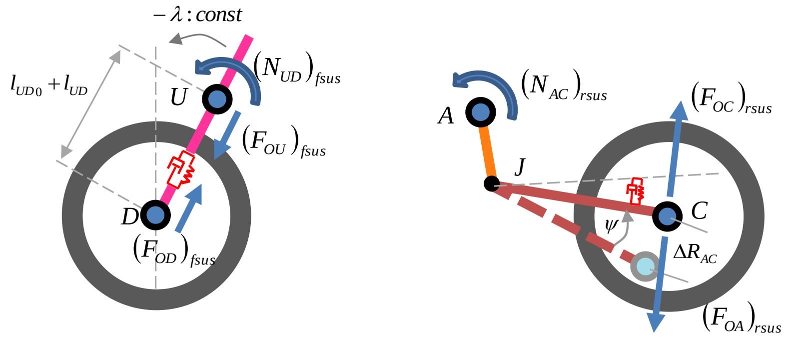

(a) Front suspension (b) Rear suspension

Figure 2 Suspension force

τ_{xp} is the lean torque from the rider's upper torso, τ_{zp} is the reaction torque of the rider's arm along with z-axis of rider's upper torso, τ_{xa} is the lean torque of the motorcycle, and τ_{zf} and τ_{zr} are self-aligning torque from the rear wheel and the front wheel. ~ describes the notation of a skew symmetric matrix for exterior product.

$\mathbf{F}_{AC}$ and $\mathbf{F}_{UD}$ are interaction caused by front and rear suspensions. Figure 2 shows the displacement of suspensions. The rear suspension force is assumed to be proportional to the displacement of rear suspension: $\Delta\mathbf{R}_{AC.}$ The front suspension force $\mathbf{F}_{AC}$ is simply described along with the z-direction of the U coordinate.

$$\mathbf{F}_{UD} = \mathbf{e}_z \cdot \left(Kds \cdot lud + Cds \cdot \dot{l}ud \right) \tag{8}$$

$$\begin{aligned} \mathbf{F}_{AC} &= C_{AJ} \cdot \mathbf{e}_z \cdot \left(-Kcs \cdot \Delta R_{AC} - Cds \cdot \Delta \dot{R}_{AC} \right) \\ &= C_{AJ} \cdot \mathbf{e}_z \cdot \left\{ Kcs \cdot \left| \mathbf{R}_{JC} \right| \cdot \sqrt{2(1-\cos\psi)} + Cds \cdot \left| \mathbf{R}_{JC} \right| \cdot \dot{\psi} \right\} \end{aligned} \tag{9}$$

$\mathbf{f}_{opr}$ and $\mathbf{f}_{opf}$ in the equation (3) are the tire forces,

$$\mathbf{f}_{cpr} = f_{cx} \cdot D_{OCxx} + f_{cy} \cdot \tilde{\mathbf{e}}_z \cdot D_{OCxx} + f_{cz} \cdot \tilde{D}_{OCxx} \cdot C_{OC} \cdot \mathbf{e}_y, \tag{10}$$

where D_{OCxx} is the unit vector of the x-direction of the rear wheel:

$$D_{OCxx} = \left(\frac{-\tilde{\mathbf{e}}_z \cdot C_{OC} \cdot \mathbf{e}_y}{\left| -\tilde{\mathbf{e}}_z \cdot C_{OC} \cdot \mathbf{e}_y \right|} \right) \quad . \tag{11}$$

In Equation (10), f_{cx} and f_{cy} are the longitudinal and the lateral tire force. As it discussed in Chapter 2, the nonlinear rider-motorcycle model has to be linearized for designing a stability control system. Referring to Magic Formula [3], [10], to include the nonlinear characteristics of tire cornering forces in the linearized model, the tire cornering forces can be expressed using hyperbolic tangent function [11]:

$$\begin{aligned} f_{cx} &= \mu_{\max} \cdot \frac{\tanh(a_\mu \cdot \varepsilon)}{a_\mu b_\mu} \cdot f_{cz}, \\ f_{cy} &= \mu_{\max} \cdot \left\{ \left(c_{S11} \frac{F_z}{g} + c_{S12} \right) \cdot \frac{\tanh(a_{c1} \cdot \beta)}{a_{c1} b_{c1}} + \left(c_{S21} \frac{F_z}{g} + c_{S22} \right) \cdot \frac{\tanh(a_{c2} \cdot \theta_x)}{a_{c2} b_{c2}} \right\} \\ &\quad \cdot \sqrt{1 - \left(\frac{f_{cx}}{f_{cx\max}} \right)^2}, \\ f_{cz} &= K_{cz} \cdot \Delta R_r + C_{cz} \cdot \Delta \dot{R}_r, \end{aligned} \tag{12}$$

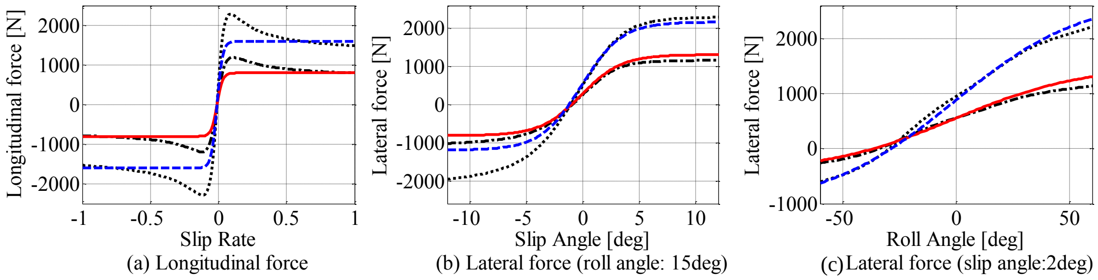

Figure 3 Characteristic of tire force

where ε is the slip rate, a_μ=25, $a_\mu \cdot b_\mu$=1, a_{c1}=16, $a_{c1} \cdot b_{c1}$=10, a_{c2}=1, $a_{c2} \cdot b_{c2}$=1.6, C_{S11}=60.64, C_{S12}=4435.84, C_{S21}=14.60, C_{S22}=73.00, K_{cz}=150000, C_{cz}=1000. Figure 3 shows the characteristic of the rear tire force given as (12) and Magic Formula. The tire forces of the front wheel are derived similarly.

2.3 Equations of Motion

With the velocity matrix H, the equation of motion is expressed

$$M_{HO} \cdot \dot{H} = F_H, \tag{13}$$

where M_{HO} and F_H represent the mass matrix and the force matrix:

$$\begin{aligned} M_{HO} &= \mathrm{diag}\left(M_A \quad J_{OA} \quad M_U \quad J_{OU} \quad M_W \quad J_{OW} \quad M_C \quad J_{OC} \quad M_D \quad J_{OD}\right) \\ F_H &= \left[\Gamma'^T_{OA} \quad \Gamma'^T_{OU} \quad \Gamma'^T_{OW} \quad \Gamma'^T_{OC} \quad \Gamma'^T_{OD}\right] \end{aligned} \tag{14}$$

$$\begin{gathered} \Gamma_{Oi} = \begin{bmatrix} \mathbf{F}'_{Oi} - \tilde{\mathbf{\Omega}}'_{Oi} \cdot M_i \cdot \mathbf{V}'_{Oi} \\ \mathbf{N}'_{Oi} - \tilde{\mathbf{\Omega}}'_{Oi} \cdot J_{Oi} \cdot \mathbf{\Omega}'_{Oi} \end{bmatrix}, \\ M_i = m_i \cdot \begin{bmatrix} 1 & 0 & 0 \\ 0 & 1 & 0 \\ 0 & 0 & 1 \end{bmatrix}, \\ J_{Oi} = \begin{bmatrix} I_{ix} & 0 & 0 \\ 0 & I_{iY} & 0 \\ 0 & 0 & I_{iZ} \end{bmatrix} \quad . \\ (i : A,\ U,\ C,\ D\ \ and\ \ W) \end{gathered} \tag{15}$$

Rewriting Equation (13) with the generalized velocity, the equation of motion is obtained as

$$M_S \cdot \dot{\mathbf{S}} = F_S. \tag{16}$$

M_S and F_S are respectively the transformed mass matrix and the transformed force matrix:

$$\begin{aligned} M_S &= \left(\frac{\partial H}{\partial S}\right)^T \cdot M_{HO} \cdot \left(\frac{\partial H}{\partial S}\right) \\ F_S &= \left(\frac{\partial H}{\partial S}\right)^T \cdot \left(F_H - M_{HO} \cdot \frac{d}{dt}\left(\frac{\partial H}{\partial S}\right) \cdot \mathbf{S}\right) \end{aligned} \tag{17}$$

From the equations (2) and (16), the nonlinear state-space description is represented:

$$\dot{\mathbf{x}} = \mathbf{A}_s(\mathbf{x})\mathbf{x} + \mathbf{B}_s(\mathbf{x})\mathbf{u} + \mathbf{E}_s(\mathbf{x}), \tag{18}$$

where

$$A_S = \begin{bmatrix} O_{12} & \dfrac{\partial \dot{\mathbf{Q}}}{\partial \mathbf{S}} \\ O_{12} & M_S^{-1} \cdot \dfrac{\partial F_S}{\partial \mathbf{S}} \end{bmatrix} = \begin{bmatrix} O_{12} & \mathrm{diag}\begin{bmatrix} C_{OA} & I_3 & 1 & 1 & 1 & 1 & 1 & 1 \end{bmatrix} \\ O_{12} & M_S^{-1} \cdot \left(-\left(\dfrac{\partial H}{\partial S} \right)^T \cdot M_{HO} \cdot \dfrac{d}{dt}\left(\dfrac{\partial H}{\partial S} \right) \right) \end{bmatrix},$$

$$B_S = \begin{bmatrix} O_{12\times 3} \\ Ms^{-1} \cdot \dfrac{\partial F_S}{\partial \mathbf{u}} \end{bmatrix}, E_S = \begin{bmatrix} O_{12\times 1} \\ Ms^{-1} \cdot F_S \end{bmatrix} .$$

The state vector **x** and the input vector **u** are given as

$$\mathbf{x} = \begin{bmatrix} \mathbf{Q} \\ \mathbf{S} \end{bmatrix}, \; \mathbf{u} = \begin{bmatrix} \tau_{rr} \\ \tau_{rf} \\ \tau_f \end{bmatrix} = \begin{bmatrix} \tau_{rr} \\ \tau_{rf} \\ \tau_{fs} + \tau_{fc} \end{bmatrix} . \tag{19}$$

3 ANALYSIS OF THE LINEARIZED STATE-SPACE MODEL

3.1 Linearized State-Space Model

To analyze eigenvalues and frequency responses, Equations (2) and (16), which give the nonlinear dynamical model, are linearized around an equilibrium point [5]. When $\mathbf{Q}_0$ and $\mathbf{S}_0$ is a set of the equilibrium point with the generalized coordinate and generalized velocity respectively, Equations (1), (2) and (17) are linearized as:

$$\begin{aligned} &\mathbf{Q} = \mathbf{Q}_0 + \Delta\mathbf{Q}, \quad \mathbf{S} = \mathbf{S}_0 + \Delta\mathbf{S}, \\ &M_S = M_{S0} + \Delta M_S, \quad F_S = F_{S0} + \Delta F_S, \\ &\frac{\partial \dot{\mathbf{Q}}}{\partial \mathbf{S}} = \left.\frac{\partial \dot{\mathbf{Q}}}{\partial \mathbf{S}}\right|_0 + \Delta \frac{\partial \dot{\mathbf{Q}}}{\partial \mathbf{S}} \end{aligned} . \tag{20}$$

Using Equation (20), Equations (2) and (16) can be linearized:

$$\Delta\dot{\mathbf{Q}} = \Delta \frac{\partial \dot{\mathbf{Q}}}{\partial \mathbf{S}} \mathbf{S}_0 + \left.\frac{\partial \dot{\mathbf{Q}}}{\partial \mathbf{S}}\right|_0 \Delta\mathbf{S}, \tag{21}$$

$$M_{S0} \cdot \Delta\dot{\mathbf{S}} = \Delta F_S . \tag{22}$$

Thus the linearized state-space description is derived

$$\Delta\dot{\mathbf{x}} = \mathbf{A}_l \Delta\mathbf{x} + \mathbf{B}_l \Delta\mathbf{u}, \tag{23}$$

where

$$A_l = \begin{bmatrix} \left.\dfrac{d}{dt}\left(\dfrac{\partial \dot{\mathbf{Q}}}{\partial \mathbf{S}} \mathbf{S}_0 \right)\right|_0 & \left.\dfrac{\partial \dot{\mathbf{Q}}}{\partial \mathbf{S}}\right|_0 \\ M_{S0}^{-1} \cdot \left.\dfrac{\partial F_S}{\partial \mathbf{Q}}\right|_0 & M_{S0}^{-1} \cdot \left.\dfrac{\partial F_S}{\partial \mathbf{S}}\right|_0 \end{bmatrix}, \quad B_l = \begin{bmatrix} O_{12\times 3} \\ M_{S0}^{-1} \cdot \left.\dfrac{\partial F_S}{\partial \mathbf{u}}\right|_0 \end{bmatrix}, \tag{24}$$

$$\Delta \mathbf{x} = \begin{bmatrix} \Delta \mathbf{Q} \\ \Delta \mathbf{S} \end{bmatrix}, \quad \Delta \mathbf{u} = \begin{bmatrix} \Delta \tau_{rr} \\ \Delta \tau_{rf} \\ \Delta \tau_{f} \end{bmatrix}. \tag{25}$$

3.2 Eigenvalue Analysis and Frequency Response Analysis

Table 2 Eigenvalue of the system matrix (Velocity: 40 km/h)

Roll angle	0 [deg]	19.7 [deg]
α_1	-1.20	-0.02
α_2	-1.98	-26.53
α_3	-4.11	-4.11
α_4	-12.43	-12.11
α_5	0.00	-0.50
β_1	-1.54 ± 3.87 i	0.12 ± 4.14 i
β_2	-25.49 ± 30.82 i	-10.97 ± 36.58 i
β_3	-1.98 ± 7.89 i	-0.27 ± 7.09 i
β_4	-7.19 ± 47.22 i	-18.52 ± 45.66 i
β_5	-1.71 ± 30.43 i	-2.58 ± 28.34 i
β_6		-2.55 ± 2.39 i

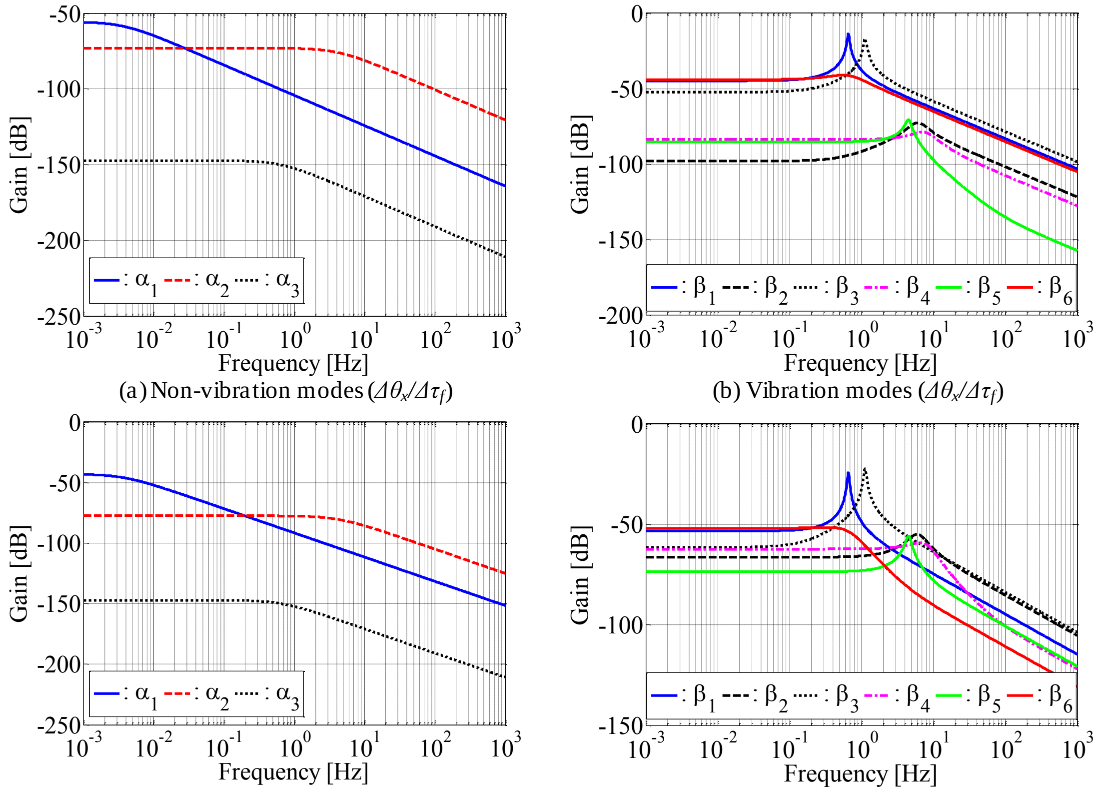

(a) Non-vibration modes ($\Delta\theta_x/\Delta\tau_f$)
(b) Vibration modes ($\Delta\theta_x/\Delta\tau_f$)
(c) Non-vibration modes ($\Delta\delta/\Delta\tau_f$)
(d) Vibration modes ($\Delta\delta/\Delta\tau_f$)

Figure 4 Frequency response of linearized steady-state circular turning model at velocity: 40 km/h, roll angle: 19.7 deg.

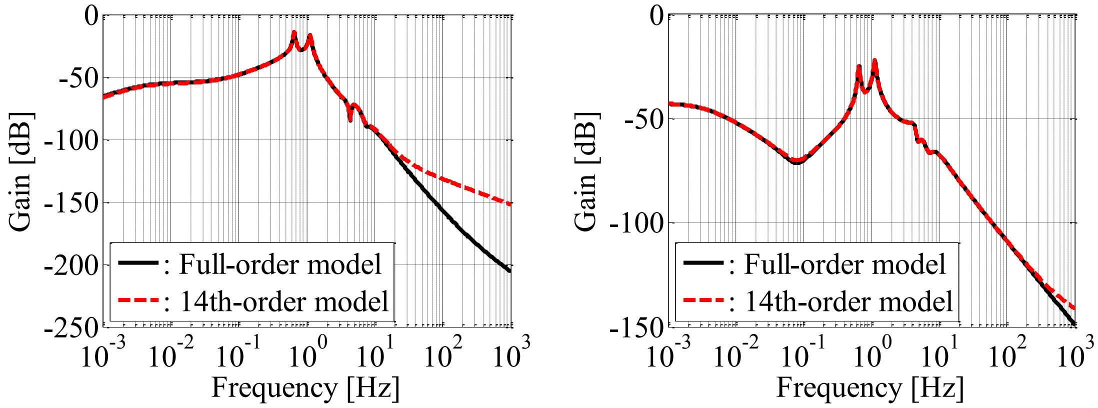

(a) Frequency responses ($\Delta\theta_x/\Delta\tau_f$) (b) Frequency responses ($\Delta\delta/\Delta\tau_f$)

Figure 5 Frequency Responses of linearized full-order and 14th-order steady-state circular turning model at velocity: 40 km/h, roll angle: 19.7 deg.

To derive a reduced-order model for designing the front-steering assist control system, the analysis is done by diagonalizing the system matrix A_l. The eigenvalues of the matrix A_l of the linearized model in straight running and circular turning at the speed of 40 km/h are shown in Table 2. Figure 4 (a) and (b) show the frequency responses of the linearized circular turning model from steering torque $\Delta\tau_f$ to the roll angle $\Delta\theta_x$. Figure 4 (c) and (d) also show the frequency responses from steering torque $\Delta\tau_f$ to the steering angle $\Delta\delta$.
Real values α_1 and α_2 are the eigenvalues of capsize modes, which are related to the roll and steering, respectively. For complex values, β_1 is the eigenvalue of the weave mode and β_2 is the eigenvalue of the wobble mode. It is seen from Table 2 that the vibration mode of β_1 is stable in circular turning while that in straight running is stable. It is also seen that the peak of the frequency responses β_3 and β_6 are close to the weave mode β_1. The frequency response β_3 is identified as the eigenvalue of the rider's upper torso mode [5]. The peak of the frequency responses β_4 and β_5 are also seen to be close to the eigenvalue of the wobble mode β_2. In Figure 4 (a) and (c), the gain of the frequency responses β_3 is small compared to α_1 and α_2. While the gain of the frequency responses β_2, β_4 and β_5 are small compared to the others in Figure 4 (b), those are not ignorable in Figure 4 (d).
From the result of frequency response analysis, ignoring the small contributors: α_3, α_4 and α_5 in Table 2, 14$_{th}$-order model is obtained as shown in Figure 5. The 14$_{th}$-order model highly consists of the full-order model below 20 Hz for $\Delta\theta_x/\Delta\tau_f$, and below 300Hz for $\Delta\delta/\Delta\tau_f$. Without suspensions, it is shown that 12$_{th}$-order model is enough to express the full-order model [5]. The 12$_{th}$order model does not include β_4.

3.3 The Front-Steering Assist Control System Design

Figure 6 shows the generalized plant to design $H\infty$ control system for the reduced-order model derived as shown in Figure 4. The feedback signal is the roll rate $\Delta\theta_x$ and the output of the designed controller is the steering torque $\Delta\tau_{fc}$.
W_S and W_T are given as Equation (26) and Equation (27), respectively. W_N is fixed to 1.

$$W_S = \frac{g_s \cdot \omega_{ns}^2}{s^2 + 2\zeta_{ds}\omega_{ds}s + \omega_{ds}^2} \tag{26}$$
$$g_s = 2.24, \quad \omega_{ns} = 36.1, \quad \zeta_{ds} = 1, \quad \omega_{ds} = 36.1,$$

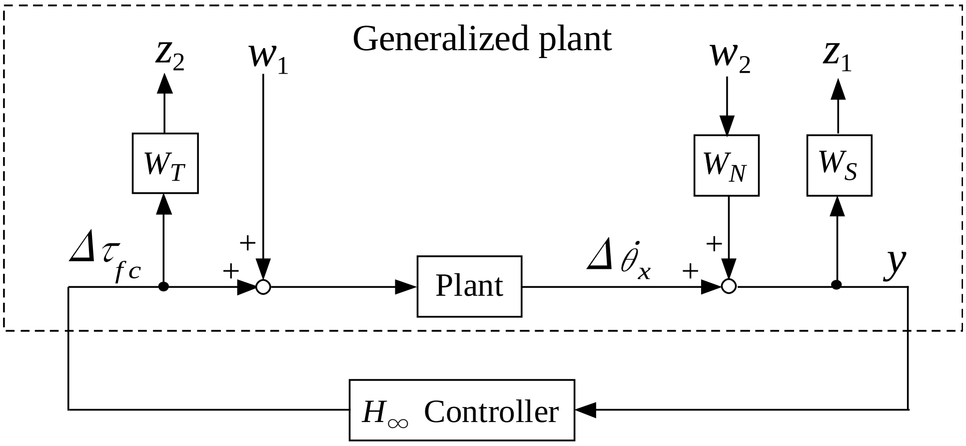

Figure 6 Generalized plant

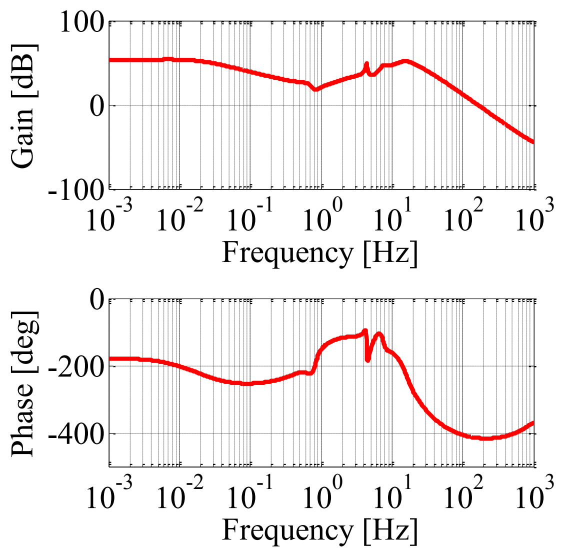

Figure 7 Bode diagram of H_∞ controller for linearized steady-state circular turning model at velocity: 40 km/h, roll angle: 19.7 deg.

$$W_T = \frac{g_t \cdot \omega_t^2}{s^2 + 2\zeta_t \omega_t s + \omega_t^2} \qquad (27)$$
$$g_t = 0.00023, \quad \omega_t = 7539.8, \quad \zeta_{dt} = 1.$$

The bode diagram of the H_∞ controller designed using W_S, W_T and W_N is shown in Figure 7.

4 SIMULATIONS

It is supposed that existence of suspension in the model mainly affects the pitch motion of the motorcycle. Thus the performance of the front-steering assist control system should be verified when the motorcycle is in pitching motion. Figure 8 shows simulation results of the modes with and without suspensions.

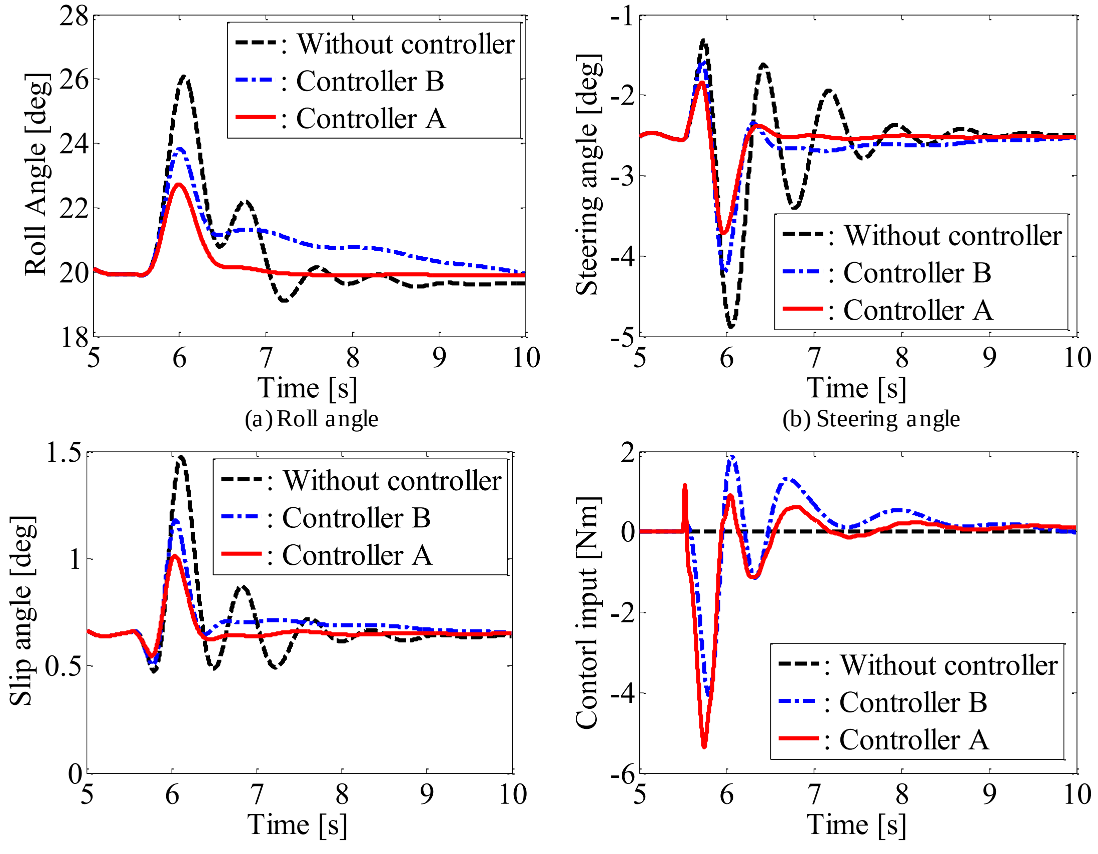

(a) Roll angle (b) Steering angle

(c) Slip Angle (d) Control input

Figure 8 Effects of suspensions in simulations

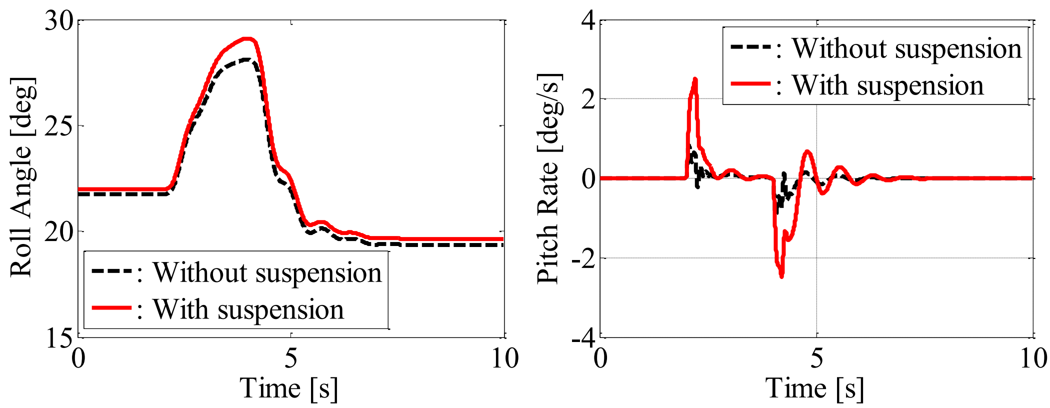

(a) Roll angle (b) Pitch rate

Figure 9 Performance of the Front Steering Assist Control

From 2 s to 4 s, 50 Nm of the braking torque is given to the front and rear wheels. The friction coefficient is 0.8. In this situation, except for braking time, the motorcycle velocity is controlled 12 by the PID control of the rear wheel torque. The initial velocity is 50 km/h and it decreases to 40 km/h after braking. During simulation, the steering torque is fixed to -6.5 Nm, which gives the roll angle 19.7 deg when the velocity is 40 km/h. Starting of braking at 2s and finishing of braking at 4s causes the pitching motion From Figure 8 (a), it is seen that braking increases the roll angle from 2 s to 4 s and oppositely releasing from braking decreases the roll angle. The roll angle of the model with suspensions varies more than that without suspensions. Figure 8 (b) shows the model with suspensions behaves by the large pitch rate than that without suspensions. To confirm the performance of the controller, an impulsive torque disturbance, which amplitude is 10 Nm and its width is 0.4 s, is given around steering axis at 5.5 sec. Other conditions are the same as the simulation shown in Figure 8. Figure 9 is the simulation result of the front-steering assist control system. Controller A is designed for the model with suspensions, while Controller B is designed for that without suspensions. When the impulsive disturbance is added, the roll angle without controller is increased 6.8 deg. As shown in Figure 9 (a), Controller A reduces the fluctuation of the roll angle 59%. Compared to Controller B, Controller A reduces the fluctuation 28.6% and settles the roll angle immediately. The steering control shown in Figure 9 (b) reduces fluctuation of the tire slip angles as shown in Figure 9 (c). Figure 9 (d) shows the input torque and its maximum value is -5.6 Nm.

5. CONCLUSIONS

Based on the multi-body dynamics theory, a dynamical model of the nonlinear twelve-degree freedom rider-motorcycle system is derived and linearized for the control design. The model consists of five rigid bodies, and includes not only the lean angle of the rider’s upper torso, but also the front and rear suspensions. This model enables consideration of pitching motion of the motorcycle caused by extension and compression of suspensions in braking situations. For circular turning at the velocity: 40 km/h, it is demonstrated that the front-steering assist control system designed for the model with suspension can immediately stabilize the motorcycle posture when the motorcycle behaves the pitching motion.

ACKNOWLEGEMENTS

This Research is a part of Global GCOE program, the Center of Education and Research of Symbiotic, Safe and Secure System Design, Keio University. Authors would like to thank all who are involved for their support.

REFERENCES

[1] V. Cossalter and R. Lot, “A motorcycle multi-body model for real time simulations based on the natural coordinates approach”, Vehicle System Dynamics, vol. 37, No.6, (2002), pp. 423-447.

[2] [R. Lot and M. DA LIO, “A symbolic approach for automatic generation of the equations of motion of multibody systems”, Multibody dynamics 12 (2004), pp. 147-172.

[3] R. S. Sharp, S. Evangelou and D.J.N. Limebeer, “Advances in the modeling of motorcycle dynamics”, Multibody dynamics 12 (2004), pp. 251-283.

[4] S. Zhu, H. Nishimura, S. Iwamatsu, H. Tajima, “Dynamical Analysis of Motorcycle by Multibody Dynamics Approach”, Journal if System Design and Dynamics, Vol. 2, No. 3, (2008), pp. 703-714

[5] S. Zhu and H. Nishimura, “An Attitude Stabilization Control System for a Motorcycle (A front-steering assist control for steady-state circular turning at the low speed)”, Transactions of the Japan Society of Mechanical Engineers, Series C, Vol. 75, No. 753 (2009), pp. 1336-1345.

[6] T. Katayama, A. Aoki, and T. Nishimi, “Control Behavior of Motorcycle Riders”, Vehicle System Dynamics 13 (1988), pp. 211-229.

[7] Y. Kamata, H. Nishimura, “System Identification and Attitude Control of Motorcycle by Computer-Aided Dynamics Analysis”, JSAE Review, Vol. 24, No.4 (2003), pp. 411-416.

[8] Y. Kamata, H. Nishimura, H. Iida, “System Identification and Front-Wheel Steering Control of Motorcycle”, Transactions of The Japan Society of Mechanical Engineers, Series C, Vol. 69, No. 688 (2003), pp. 3191-3197.

[9] JSAE Technical Report Series 25, “The Dynamic Characteristic of Motorcycle”, and Its Environment, Society of Automotive Engineers of Japan, Inc., (1984)

[10] H. B. Pacejka, “Tyre and Vehicle Dynamics”, Butterworth and Heinemann, Oxford, 2002.

[11] S. Murakami. S. Zhu, H. Nishimura, “Validation of a Front-Steering Assist Control for a Motorcycle”, JSAE Dynamics and Design Conference 2010, 323.pdf, (2010)

[12] S. Miyasaka, T. Fukao, N. Adachi, “Hybrid Control System Design for Active Steering”, JSAE Dynamics and Design Conference 2004, 224.pdf, (2004)